Published in final edited form as:
Methods Enzymol. 2006 ; 413: 103–122.

Characterization of Amyloid Structures at the Molecular Level by Solid State Nuclear Magnetic Resonance Spectroscopy

Robert Tycko
Laboratory of Chemical Physics, National Institute of Diabetes and Digestive and Kidney Diseases, National Institutes of Health, Building 5, Room 112, Bethesda, Maryland 20892-0520, e-mail: robertty@mail.nih.gov, phone: 301-402-8272, fax: 301-496-0825

Abstract

Solid state nuclear magnetic resonance (NMR) spectroscopy is particularly useful in structural studies of amyloid fibrils because solid state NMR techniques have unique capabilities as site-specific, molecular-level structural probes of noncrystalline materials. These techniques provide experimental data that strongly constrain the secondary, tertiary, and quaternary structures of amyloid fibrils, permitting the development of experimentally-based structural models. Examples of techniques that are applicable to amyloid samples prepared with isotopic labeling of specific sites and to samples prepared with uniform isotopic labeling of selected residues are presented, illustrating the utility of the various techniques and labeling schemes. Information regarding the preparation of amyloid samples for solid state NMR measurements is also included.

I. Introduction

The phrase “solid state NMR” simply means nuclear magnetic resonance (NMR) techniques that are applicable to samples that are solids (crystalline or noncrystalline) or solid-like (*e.g.*, phospholipid bilayer membranes, precipitated protein aggregates). As demonstrated by recent studies in our laboratory (Antzutkin *et al*., 2000; Antzutkin *et al*., 2003; Antzutkin *et al*., 2002; Balbach *et al*., 2000; Balbach *et al*., 2002; Gordon *et al*., 2004; Oyler and Tycko, 2004; Petkova *et al*., 2004; Petkova *et al*., 2002; Petkova *et al*., 2005; Tycko and Ishii, 2003) and in other laboratories (Benzinger *et al*., 1998; Benzinger *et al*., 2000; Burkoth *et al*., 2000; Gregory *et al*., 1998; Heller *et al*., 1996; Jaroniec *et al*., 2002b; Jaroniec *et al*., 2004; Kammerer *et al*., 2004; Lansbury *et al*., 1995; Laws *et al*., 2001; Naito *et al*., 2004; Siemer *et al*., 2005), amyloid fibrils are excellent systems for solid state NMR investigations. This is because (i) amyloid fibrils, although noncrystalline, do have well-defined molecular structures and therefore yield solid state NMR data that are of high quality and have clear interpretations, (ii) amyloid fibrils can be prepared with selective or uniform isotopic labeling in the multimilligram quantities required for most solid state NMR measurements, (iii) amyloid fibrils can be prepared in high concentrations by lyophilization or centrifugation, leading to good signal-to-noise ratios in the solid state NMR data, (iv) the structural information available from solid state NMR measurements is arguably more direct and specific than information available from other measurements, and (v) the molecular structures of amyloid fibrils are of great current interest in the biomedical, biophysical, and biochemical research communities.

Based on x-ray fiber diffraction data, we know that the principal structural motifs in amyloid fibrils are cross-β motifs, *i.e.*, ribbon-like β-sheets extending over the length of the fibrils, comprised of β-strand peptide segments oriented approximately perpendicular to the long fibril

prepared for *Methods in Enzymology* volume on “Amyloid, Prions, and Other Protein Aggregates, Part B”, edited by R. Wetzel and I. Kheterpal

axis and linked by backbone hydrogen bonds oriented approximately parallel to the long axis (Sunde and Blake, 1998; Tycko, 2004). The reality of the cross-β motif in fibrils formed by the β-amyloid peptide associated with Alzheimer's disease (Aβ) has been confirmed by electron microscopy (EM) (Serpell and Smith, 2000) and by recent solid state NMR measurements on oriented fibrils (Oyler and Tycko, 2004). Given that amyloid fibrils are constructed from β-sheets, the molecular structures of amyloid fibrils can be discussed at the levels of primary, secondary, tertiary, and quaternary structure, in analogy to the classification of structure in globular proteins and protein complexes. Primary structure refers to the amino acid sequence. For amyloid fibrils, secondary structure refers to the locations of β-strand and non-β-strand segments and of ordered and disordered segments. Tertiary structure refers to the arrangement of β-strands into parallel or antiparallel β-sheets. Quaternary structure refers to the relative orientation of and contacts between β-sheets. As explained below, solid state NMR data can be used to determine or place strong constraints on secondary, tertiary, and quaternary structure in amyloid fibrils. These constraints permit the development of complete structural models based entirely on experimental data (Burkoth *et al*., 2000; Jaroniec *et al*., 2004; Kammerer *et al*., 2004; Lansbury *et al*., 1995; Petkova *et al*., 2002).

II. Determination of secondary structure

Constraints on secondary structure come from at least two types of solid state NMR measurements. One approach is simply to measure isotropic ^{13}C NMR chemical shifts in fibrils that are prepared with ^{13}C labels at specific carbonyl, α-carbon, or β-carbon si tes (Balbach *et al*., 2002; Heller *et al*., 1996; Laws *et al*., 2001; Naito *et al*., 2004) or with uniformly ^{13}C-labeled residues (Balbach *et al*., 2000; Jaroniec *et al*., 2002b; Jaroniec *et al*., 2004; Petkova *et al*., 2004; Petkova *et al*., 2002; Petkova *et al*., 2005; Siemer *et al*., 2005). In β-strand segments, carbonyl and α-carbon lines are shifted upfield relative to “random coil” chemical shift values, while β-carbon lines are shifted downfield (Balbach *et al*., 2000; Petkova *et al*., 2002; Saito, 1986; Spera and Bax, 1991; Wishart *et al*., 1991). Observation of β-strand-like ^{13}C chemical shifts for several sequential residues provides strong evidence for a β-strand encompassing these residues. As an example, ^{13}C chemical shift data for $A\beta_{16\text{-}22}$ fibrils (where $A\beta_{n\text{-}m}$ means residues n through m of the Aβ peptide) are plotted in Fig. 1 as “secondary shifts”, or the differences between observed chemical shifts and the corresponding random coil shifts.

The chemical shift measurements are carried out with magic-angle spinning (MAS), a standard solid state NMR technique in which samples are placed in cylindrical capsules (called MAS rotors) and spun rapidly about an axis that makes an angle $\theta_m \equiv \cos^{-1}(1/\sqrt{3})$ with the magnetic field of the NMR spectrometer, using a pneumatic turbine system. MAS at 5-25 kHz frequencies averages out both chemical shift anisotropies (CSA) and nuclear magnetic dipole-dipole couplings (*e.g.*, between ^{13}C-^{13}C and ^{15}N-^{13}C pairs), resulting in relatively sharp NMR lines at the isotropic chemical shift positions. Dipole-dipole couplings to protons are not removed efficiently by MAS at readily achievable spinning frequencies and therefore must be removed by high-power proton decoupling. In the case of samples with uniformly labeled residues, two-dimensional (2D) spectroscopy (or higher-dimensional spectroscopy) is usually required for resolution and assignment of the ^{13}C MAS NMR lines (Balbach *et al*., 2000; Jaroniec *et al*., 2002b; Jaroniec *et al*., 2004; Petkova *et al*., 2004; Petkova *et al*., 2002; Petkova *et al*., 2005; Siemer *et al*., 2005). Fig. 2 shows examples of 2D solid state ^{13}C-^{13}C NMR spectra of $A\beta_{1\text{-}40}$ fibrils, synthesized with uniform ^{15}N and ^{13}C labeling of selected residues.

A more sophisticated and potentially more powerful approach is to use a class of solid state NMR techniques that are collectively called “tensor correlation methods” (Blanco and Tycko, 2001; Chan and Tycko, 2003; Costa *et al*., 1997a; Costa *et al*., 1997b; Dabbagh *et al*., 1994; Feng *et al*., 1997; Feng *et al*., 1996; Ishii *et al*., 1996; McDermott *et al*., 1994; Reif *et al*., 2000; SchmidtRohr, 1996a; SchmidtRohr, 1996b; Takegoshi *et al*., 2000; Tycko and Dabbagh,

1991; Weliky *et al*., 1993; Weliky and Tycko, 1996). These techniques provide quantitative constraints on the relative orientations of pairs of chemical bonds (*e.g.*, the relative orientation of a ^{15}N-H bond and a $^{13}C_{\alpha}$-H bond within one residue, which depends on the backbone ϕ torsion angle for this residue) or pairs of functional groups (*e.g.*, the relative orientation of sequential ^{13}C-labeled backbone carbonyl sites, which depends on the backbone ϕ and ψ torsion angles between the labeled sites). Tensor correlation methods are particularly useful for determining sidechain conformations or backbone conformations at residues where the chemical shift data suggest a non-β-strand conformation (Antzutkin *et al*., 2003).

Structurally ordered segments in amyloid fibrils can be distinguished from disordered segments by measurements of ^{13}C MAS NMR linewidths. In lyophilized samples, ordered segments exhibit linewidths of roughly 2 ppm or less for backbone sites, while disordered segments exhibit linewidths greater than 3 ppm (Balbach *et al*., 2000; Petkova *et al*., 2004; Petkova *et al*., 2002). For comparison, solid state ^{13}C MAS NMR linewidths for peptides that are tightly bound to antibodies, and are therefore structurally ordered, are 1.5-2.5 ppm in noncrystalline frozen solutions (Sharpe *et al*., 2004; Weliky *et al*., 1999). Fully hydrated amyloid samples may exhibit narrower lines for ordered segments (although not necessarily), and may exhibit missing signals for disordered segments that undergo large-amplitude motions when hydrated (Jaroniec *et al*., 2002b; Jaroniec *et al*., 2004; Petkova *et al*., 2004; Siemer *et al*., 2005). Fig. 3 shows ^{13}C NMR linewidth data extracted from 2D spectra of $A\beta_{1\text{-}40}$ fibrils.

To date, helical secondary structure has not been observed in amyloid fibrils by solid state NMR, although helical segments in peptides and proteins can be identified by either ^{13}C NMR chemical shift measurements (Havlin and Tycko, 2005) or tensor correlation methods (Blanco *et al*., 2001; Blanco and Tycko, 2001; Chan and Tycko, 2003; Long and Tycko, 1998). Solid state NMR can also be used to characterize β-turn conformations (Ashida *et al*., 2002; Sharpe *et al*., 2004; Weliky *et al*., 1999; Yao and Hong, 2004). Recent models for amyloid fibrils derived from solid state NMR and other data (Guo *et al*., 2004; Jimenez *et al*., 2002; Petkova *et al*., 2002; Williams *et al*., 2004) assign the observed non-β-strand segments to “bend” or “loop” structures, rather than the standard β-turns invoked in some earlier models (George and Howlett, 1999; Lazo and Downing, 1998; Li *et al*., 1999).

III. Determination of tertiary structure

As reflected in structural models for Aβ fibrils published before 2000 (Chaney *et al*., 1998; George and Howlett, 1999; Lazo and Downing, 1998; Li *et al*., 1999), a consensus once existed that the cross-β motifs in amyloid fibrils were comprised of antiparallel β-sheets. This belief was overturned by solid state NMR studies of $A\beta_{10\text{-}35}$ fibrils by Lynn, Meredith, Botto, and coworkers (Benzinger *et al*., 1998; Benzinger *et al*., 2000; Burkoth *et al*., 2000; Gregory *et al*., 1998), which showed that $A\beta_{10\text{-}35}$ fibrils contain only in-register parallel β-sheets (*i.e.*, β-sheets in which residue k in one β-strand forms backbone hydrogen bonds with residues k-1 and k+1 of a neighboring β-strand). Subsequently, in-register parallel β-sheets have been discovered in other amyloid fibrils, including full-length Aβ fibrils (Antzutkin *et al*., 2000; Antzutkin *et al*., 2002; Balbach *et al*., 2002; Petkova *et al*., 2005; Torok *et al*., 2002), by solid state NMR (Antzutkin *et al*., 2000; Antzutkin *et al*., 2002; Balbach *et al*., 2002; Gordon *et al*., 2004) and other techniques (Der-Sarkissian *et al*., 2003; Jayasinghe and Langen, 2004; Torok *et al*., 2002). However, certain amyloid fibrils have been shown to contain antiparallel β-sheets, particularly fibrils formed by relatively short peptides (Balbach *et al*., 2000; Gordon *et al*., 2004; Kammerer *et al*., 2004; Lansbury *et al*., 1995; Petkova *et al*., 2004), implying that there is no truly universal molecular structure for amyloid fibrils. Results obtained to date suggest that parallel β-sheets are favored in amyloid fibrils because parallel alignment of β-strand segments maximizes hydrophobic contacts (Antzutkin *et al*., 2000; Petkova *et al*., 2002) and permits favorable interactions among polar sidechains, dubbed “polar zippers” by

M.F. Perutz (Perutz *et al*., 1994), within a single β-sheet. Antiparallel β-sheets can be favored by electrostatic interactions, but have been found in amyloid fibrils comprised of peptides with hydrophobic segments only when the requirement for optimal hydrophobic contacts can also be met with antiparallel alignment of β-strand segments (Balbach *et al*., 2000; Gordon *et al*., 2004; Lansbury *et al*., 1995; Petkova *et al*., 2004).

Constraints on tertiary structure are obtained from measurements of nuclear magnetic dipole-dipole couplings, whose strength is proportional to $\gamma_I\gamma_S/r_{IS}^3$, where γ_I and γ_S are the gyromagnetic ratios of coupled nuclei I and S and R_{IS} is the internuclear distance. For a ^{13}C-^{13}C pair at R_{IS} = 4.8 Å (the interstrand distance in a β-sheet), the coupling strength is 69 Hz, implying a 15 ms time scale for evolution of NMR signals from ^{13}C nuclei with 4.8 Å separations. For a ^{15}N-^{13}C pair at R_{IS} = 4.1 Å (the approximate distance between an amide nitrogen and a carbonyl carbon in an interstrand hydrogen bond), the coupling strength is 45 Hz, implying a 22 ms time scale.

In-register parallel β-sheets can be identified by synthesizing a series of peptide samples with single ^{13}C labels at backbone or sidechain sites (Antzutkin *et al*., 2000; Balbach *et al*., 2002; Benzinger *et al*., 1998; Gregory *et al*., 1998). Because carbonyl and methyl carbon sites have relatively weak dipole-dipole couplings to proteins and hence exhibit relatively long transverse spin relaxation times (T_2 values) under typical experimental conditions, it has proven most useful to label backbone carbonyl and alanine methyl sites. Measurements of intermolecular ^{13}C-^{13}C dipole-dipole couplings, as in Fig. 4 for $A\beta_{1\text{-}40}$ fibrils, permit intermolecular distances up to at least 6 Å to be measured with approximately ±10% accuracy (limited by effects of T_2 relaxation and pulse sequence imperfections). Measurements of intermolecular distances between backbone carbonyl sites alone may be incapable of distinguishing in-register alignment of β-strands from a one-residue shift in alignment, as examination of molecular models for parallel β-sheets shows that a one-residue shift only increases the nearest-neighbor intermolecular distances for backbone carbonyl labels from 4.8 Å to approximately 5.2 Å. However, nearest-neighbor intermolecular distances for alanine methyl carbon labels increase from 4.8 Å to approximately 6.7 Å with a one-residue shift. Therefore, data such as those in Fig. 4 can only be explained by an in-register parallel β-sheet structure.

Data in Fig. 4 were obtained under MAS, using a pulse sequence technique called “constant-time finite-pulse radiofrequency-driven recoupling” (fpRFDR-CT) (Balbach *et al*., 2002;Ishii *et al*., 2001). This technique is one example of a class of solid state NMR methods called “recoupling” techniques, in which radiofrequency pulses are applied in synchrony with sample rotation to restore dipole-dipole couplings or other nuclear spin interactions that would otherwise be averaged out by MAS (Bennett *et al*., 1998;Gullion and Schaefer, 1989;Gullion and Vega, 1992;Hohwy *et al*., 1998;Ishii, 2001;Mehta *et al*., 1996;Meier and Earl, 1986;Tycko and Dabbagh, 1990;Tycko *et al*., 1989). The fpRFDR-CT technique has the advantages of being relatively insensitive to T_2 effects, compatible with high-speed MAS, and effective even in the presence of the large ^{13}C CSA characteristic of carbonyl carbons.

NMR signal decay curves recorded under fpRFDR-CT or other dipolar recoupling techniques are primarily determined by the shortest internuclear distances, *i.e.*, the strongest dipole-dipole couplings. Thus, these data do not readily distinguish a *propagating* in-register parallel β-sheet structure from, for example, a structure that alternates between in-register parallel and antiparallel (or shifted) alignment of neighboring β-strands. Multiple quantum ^{13}C NMR measurements, which are sensitive to the entire network of dipole-dipole couplings among many ^{13}C spins, can distinguish among these and other structures (Antzutkin *et al*., 2000). Multiple quantum ^{13}C NMR data show that the in-register parallel alignment of peptide chains

in $A\beta_{1-40}$ fibrils extends over at least four successive peptide chains in the β-sheets (and probably hundreds of β-strands).

Antiparallel β-sheets have also been demonstrated by solid state NMR to exist in amyloid fibrils. Measurements of either ^{13}C-^{13}C (Lansbury *et al*., 1995) or ^{15}N-^{13}C (Balbach *et al*., 2000; Gordon *et al*., 2004; Kammerer *et al*., 2004; Petkova *et al*., 2004) intermolecular dipole-dipole couplings can be used to identify antiparallel β-sheets in samples with selective isotopic labeling. Measurements of intermolecular couplings between ^{15}N-labeled backbone amide sites and ^{13}C-labeled backbone carbonyl sites, using the rotational echo double resonance (REDOR) recoupling technique (Anderson *et al*., 1995; Gullion and Schaefer, 1989), are particularly powerful because the 4.1 Å internuclear distance for hydrogen bonded backbone amide and carbonyl sites is significantly shorter than other intermolecular distances in β-sheets. REDOR data such as those in Fig. 5 establish the registry of hydrogen bonds unambiguously.

Constraints on secondary and tertiary structure from fpRFDR-CT, multiple quantum NMR, REDOR, and related solid state NMR measurements can be analyzed quantitatively by comparison of experimental data with accurate numerical simulations of the solid state NMR measurements. Such simulations contain no adjustable parameters other than the geometric parameters that describe the molecular structure, such as internuclear distances.

In samples with multiple uniformly labeled residues (or multiple residues ^{13}C-labeled at α-carbons), the hydrogen bond registry in antiparallel β-sheets can also be established from 2D solid state ^{13}C NMR spectra in which transfer of nuclear spin polarization between ^{13}C-labeled sites occurs in three steps: (i) transfer from ^{13}C nuclei to directly bonded protons; (ii) transfer among protons that are within approximately 3 Å of one another; (iii) transfer from protons to directly bonded ^{13}C nuclei. Such “proton-mediated” transfers are particularly efficient for α-carbons that are directly opposite one another in antiparallel β-sheets, because the corresponding interstrand β-proton distances are approximately 2.1 Å. Proton-mediated 2D ^{13}C-^{13}C exchange spectra of antiparallel β-sheet structures therefore show strong, nonsequential crosspeaks connecting NMR lines of α-carbons that align with one another (Petkova *et al*., 2004; Tycko and Ishii, 2003). Fig. 6 shows examples of proton-mediated 2D spectra for $A\beta_{11-25}$ fibrils prepared at pH 2.4 and pH 7.4. These spectra reveal that the hydrogen bond registry is pH-dependent, presumably due to variations in electrostatic interactions.

IV. Determination of quaternary structure

Experimental constraints on quaternary structure from solid state NMR take the form of measurements of approximate distances, or “contacts”, between sidechains that project above or below the β-sheets, or between sidechain and backbone sites. Because the shortest distances between backbone atoms in different β-sheets are roughly 8 Å or more, corresponding to ^{13}C-^{13}C dipole-dipole couplings of 15 Hz or less, constraints on quaternary structure can not be obtained readily from backbone-backbone couplings.

Semi-quantitative information about sidechain-sidechain distances can be obtained from 2D ^{13}C-^{13}C exchange spectra of amyloid fibril samples with multiple uniformly labeled residues, obtained under MAS and with exchange periods greater than 100 ms. An example is shown in Fig. 7. Under these conditions, all possible intraresidue crosspeaks are observed (rather than only the one-bond or two-bond crosspeaks that appear with shorter exchange periods, as in Fig. 2), and many inter-residue crosspeaks are observed for sequential pairs of labeled residues. In addition, nonsequential crosspeaks that can only arise from quaternary contacts may be observed. Because of the complexity of the dipole-dipole coupling networks in such measurements, internuclear distances can not be determined precisely from the crosspeak intensities. However, basic principles of nuclear spin interactions (Tycko and

Dabbagh, 1992) imply that detectable crosspeaks in 2D ^{13}C exchange spectra with exchange periods less than one second can only occur if the internuclear distances are less than 10 Å.

Constraints on quaternary structure in amyloid fibrils can also be obtained from measurements of ^{15}N-^{13}C dipole-dipole couplings. Two-dimensional ^{15}N-^{13}C transferred echo double resonance (TEDOR) techniques (Hing *et al*., 1992; Jaroniec *et al*., 2002a; Michal and Jelinski, 1997) are particularly useful for detecting the proximity of specific sidechain carbon sites to specific backbone nitrogen sites in samples with multiple uniformly labeled residues. An example is shown in Fig. 8. By comparing 2D ^{15}N-^{13}C TEDOR spectra of samples in which all molecules are isotopically labeled with spectra of samples in which labeled molecules are diluted in unlabeled molecules (prior to fibril formation), one can distinguish intermolecular ^{15}N-^{13}C contacts from intramolecular contacts.

V. Construction of molecular models based on solid state NMR data

In principle, the molecular structures of amyloid fibrils can be determined completely from solid state NMR data, with no assistance from other experimental techniques, in analogy to approaches commonly employed to determined complete structures of soluble proteins from solution NMR data. However, this approach would require solid state NMR constraints on many torsion angles and many internuclear distances (both intramolecular and intermolecular) for each residue in the amyloid-forming peptide or protein. The limited resolution and signal-to-noise in solid state NMR spectra and the difficulty of preparing fibril samples with arbitrary isotopic labeling patterns make this approach impractical, except possibly in the case of fibrils formed by relatively short peptides (Jaroniec *et al*., 2004).

Fortunately, information from other experimental techniques greatly simplifies the task of constructing realistic models for amyloid fibril structures. The fact that amyloid fibrils contain cross-β motifs implies that the number of possible quaternary structures is not large, once solid state NMR data that constrain the secondary and tertiary structures are available. This is because the cross-β motif requires that all β-strand segments be approximately perpendicular to a single axis (the long axis of the fibrils), with their backbone carbonyl and amide groups orientated to permit hydrogen bonds that are approximately parallel to the same axis. The number of possible quaternary structures is also strongly restricted by measurements of fibril dimensions in EM or atomic force microscope (AFM) images and by measurements of the mass-per-length of amyloid fibrils by scanning transmission electron microscopy (Antzutkin *et al*., 2002; Goldsbury *et al*., 2000; Petkova *et al*., 2005). In addition, the structural model should make sense from the standpoint of physical chemistry (*e.g.*, exposure of hydrophobic groups to aqueous solvent should be minimized and burial of unpaired charges in the fibril core should be avoided). Detection of a small number of unambiguous contacts between β-sheets by solid state NMR may then be sufficient to determine the correct quaternary structure and hence the principal features of the full molecular structure. The precise details of sidechain conformations and backbone conformations at certain sites may remain undetermined, but these can be constrained by subsequent solid state NMR measurements as required.

These remarks apply to the determination of structural models for the cores of amyloid fibrils. As demonstrated definitively by biochemical experiments on yeast prion protein fibrils (Baxa *et al*., 2002), amyloid fibrils formed by large proteins can contain highly structured globular domains outside the fibril core. Determination of the structures of these domains in the context of amyloid fibrils would depend on solid state NMR strategies demonstrated recently in studies of microcrystalline globular proteins (Castellani *et al*., 2003; Lange *et al*., 2005).

Atomic coordinates for molecular models derived from solid state NMR constraints can be generated with molecular modeling and molecular dynamics (MD) software (Petkova *et al*., 2002). A relatively simple approach to the generation of atomic coordinates that reflect the

experimental information consists of three steps: (i) construction of a peptide in a conformation that is approximately consistent with available data by manual assignment of backbone torsion angles, using molecular modeling software; (ii) construction of an initial model for a segment of the amyloid structure by manual combination of multiple copies of this peptide with appropriate translations and rotations; (iii) refinement of the model by alternating cycles of energy minimization and MD simulations, using appropriate software. In the energy minimization and MD simulations, experimental constraints on internuclear distances and on backbone and sidechain torsion angles are enforced by artificial harmonic potential functions. If the simulations are performed without explicit solvent, electrostatic interactions are turned off or attenuated by setting the dielectric constant to an artificially large value. To identify aspects of the structural model that are not restricted by experimental constraints, the MD simulations can be run at elevated temperatures and the results of multiple independent refinement attempts can be compared. Portions of the structure that are not constrained by experiments will appear to be disordered.

VI. Sample preparation for solid state NMR

Amyloid fibrils are typically prepared by incubation of peptides or proteins in aqueous or mixed solvents under controlled conditions of concentration, pH, ionic strength, and temperature. Formation of fibrils can be monitored by EM or AFM imaging of aliquots of the incubating solution. However, it is important to recognize that EM and AFM images do not necessarily show all aggregated structures (nonfibrillar as well as fibrillar) in the solution. Ultimately, only the absence of signals attributable to nonfibrillar components in the solid state NMR spectra themselves is proof that the sample is fully fibrillized. Complete conversion to fibrils is essential because all immobilized molecules in the sample will contribute approximately equally to the solid state NMR signals. Unlike EM and AFM, solid state NMR sees the entire sample.

Structural studies of amyloid fibrils using the techniques discussed above require roughly 1 μmole of isotopically labeled molecules to achieve an adequate signal-to-noise ratio in the data. With 1 μmole samples, 2D spectra are typically obtained in 0.5-10 days (depending on the details of the measurements) when the experiments are performed at room temperature and in 9.4 T or 14.1 T magnetic fields. Solid state NMR measurements can be performed either on centrifuged pellets of fibrils or on lyophilized samples. We find that pelleted and lyophilized samples have identical chemical shifts in ^{13}C MAS NMR spectra (Petkova *et al*., 2004), indicating that lyophilization does not perturb the structures of amyloid fibrils. Certain sidechain ^{13}C NMR linewidths are reduced in hydrated samples (either pelleted or lyophilized and subsequently rehydrated) relative to the linewidths in dry lyophilized samples, most likely reflecting sidechain motions in hydrated samples that are quenched in dry samples. Lyophilization permits a denser packing of fibrils into the MAS rotors, increasing the signal-to-noise ratio and facilitating high-speed MAS. Lyophilization also minimizes sample heating by radiofrequency pulses during NMR experiments.

EM images often show several distinct morphologies for fibrils that are formed by a single peptide or protein (Goldsbury *et al*., 2000; Jimenez *et al*., 2002). The distinct morphologies may differ in diameter, twist periodicity, and apparent propensity for lateral association. The sensitivity of ^{13}C NMR chemical shifts to subtle variations in molecular structure has allowed us to demonstrate that distinct fibril morphologies have different underlying molecular structures (Petkova *et al*., 2005). The molecular structure propagates with the morphology when sonicated fibril fragments are used to seed the growth of new fibrils. Existing data suggest that fibrils with different morphologies have different quaternary structures and different conformations in non-β-strand segments. These findings imply that careful attention must be paid to fibril growth conditions, which can affect the relative abundances of various fibril

polymorphs, and to the detailed appearance of fibrils in EM images before comparisons of structural data from different research groups are made. The most definitive proof that two different groups are studying the same fibril structure would be that the two groups observe the same sets of NMR chemical shifts in their samples.

Acknowledgements

This work was supported by the Intramural Research Program of the National Institute of Diabetes and Digestive and Kidney Diseases and by the Intramural AIDS Targeted Antiviral Program of the National Institutes of Health. Data presented in the figures were obtained by Drs. Yoshitaka Ishii, Aneta T. Petkova, and John J. Balbach. Additional contributions to this work by Drs. Oleg N. Antzutkin, Richard D. Leapman, Stephen C. Meredith, David J. Gordon, Nathan A. Oyler, Jerry C.C. Chan, Gerd Buntkowsky, Anant K. Paravastu, Simon J. Sharpe, and Wai-Ming Yau are gratefully acknowledged.

References

Anderson RC, Gullion T, Joers JM, Shapiro M, Villhauer EB, Weber HP. Conformation of 1-^{13}C, ^{15}N acetyl-l-carnitine: Rotational echo double resonance nuclear magnetic resonance spectroscopy. J. Am. Chem. Soc 1995;117:10546–10550.

Antzutkin ON, Balbach JJ, Leapman RD, Rizzo NW, Reed J, Tycko R. Multiple quantum solid state NMR indicates a parallel, not antiparallel, organization of β-sheets in Alzheimer's β-amyloid fibrils. Proc. Natl. Acad. Sci. U. S. A 2000;97:13045–13050. [PubMed: 11069287]

Antzutkin ON, Balbach JJ, Tycko R. Site-specific identification of non-β-strand conformations in Alzheimer's β-amyloid fibrils by solid state NMR. Biophys. J 2003;84:3326–3335. [PubMed: 12719262]

Antzutkin ON, Leapman RD, Balbach JJ, Tycko R. Supramolecular structural constraints on Alzheimer's β-amyloid fibrils from electron microscopy and solid state nuclear magnetic resonance. Biochemistry 2002;41:15436–15450. [PubMed: 12484785]

Ashida J, Ohgo K, Asakura T. Determination of the torsion angles of alanine and glycine residues of bombyx mori silk fibroin and the model peptides in the silk I and silk II forms using 2D spin diffusion solid state NMR under off magic angle spinning. J. Phys. Chem. B 2002;106:9434–9439.

Balbach JJ, Ishii Y, Antzutkin ON, Leapman RD, Rizzo NW, Dyda F, Reed J, Tycko R. Amyloid fibril formation by $A\beta_{16\text{-}22}$, a seven-residue fragment of the Alzheimer's β-amyloid peptide, and structural characterization by solid state NMR. Biochemistry 2000;39:13748–13759. [PubMed: 11076514]

Balbach JJ, Petkova AT, Oyler NA, Antzutkin ON, Gordon DJ, Meredith SC, Tycko R. Supramolecular structure in full-length Alzheimer's β-amyloid fibrils: Evidence for a parallel β-sheet organization from solid state nuclear magnetic resonance. Biophys. J 2002;83:1205–1216. [PubMed: 12124300]

Baxa U, Speransky V, Steven AC, Wickner RB. Mechanism of inactivation on prion conversion of the Saccharomyces cerevisiae Ure2 protein. Proc. Natl. Acad. Sci. U. S. A 2002;99:5253–5260. [PubMed: 11959975]

Bennett AE, Rienstra CM, Griffiths JM, Zhen WG, Lansbury PT, Griffin RG. Homonuclear radiofrequency-driven recoupling in rotating solids. J. Chem. Phys 1998;108:9463–9479.

Benzinger TLS, Gregory DM, Burkoth TS, Miller-Auer H, Lynn DG, Botto RE, Meredith SC. Propagating structure of Alzheimer's β-amyloid(10-35) is parallel β-sheet with residues in exact register. Proc. Natl. Acad. Sci. U. S. A 1998;95:13407–13412. [PubMed: 9811813]

Benzinger TLS, Gregory DM, Burkoth TS, Miller-Auer H, Lynn DG, Botto RE, Meredith SC. Two-dimensional structure of β-amyloid(10-35) fibrils. Biochemistry 2000;39:3491–3499. [PubMed: 10727245]

Blanco FJ, Hess S, Pannell LK, Rizzo NW, Tycko R. Solid-state NMR data support a helix-loop-helix structural model for the N-terminal half of HIV-1 Rev in fibrillar form. J. Mol. Biol 2001;313:845–859. [PubMed: 11697908]

Blanco FJ, Tycko R. Determination of polypeptide backbone dihedral angles in solid state NMR by double quantum ^{13}C chemical shift anisotropy measurements. J. Magn. Reson 2001;149:131–138.

Burkoth TS, Benzinger TLS, Urban V, Morgan DM, Gregory DM, Thiyagarajan P, Botto RE, Meredith SC, Lynn DG. Structure of the β-amyloid(10-35) fibril. J. Am. Chem. Soc 2000;122:7883–7889.

Castellani F, van Rossum BJ, Diehl A, Rehbein K, Oschkinat H. Determination of solid state NMR structures of proteins by means of three-dimensional ^{15}N-^{13}C-^{13}C dipolar correlation spectroscopy and chemical shift analysis. Biochemistry 2003;42:11476–11483. [PubMed: 14516199]

Chan JCC, Tycko R. Solid state NMR spectroscopy method for determination of the backbone torsion angle psi in peptides with isolated uniformly labeled residues. J. Am. Chem. Soc 2003;125:11828–11829. [PubMed: 14505399]

Chaney MO, Webster SD, Kuo YM, Roher AE. Molecular modeling of the $A\beta_{1-42}$ peptide from Alzheimer's disease. Protein Eng 1998;11:761–767. [PubMed: 9796824]

Costa PR, Gross JD, Hong M, Griffin RG. Solid state NMR measurement of psi in peptides: A NCCN 2Q-heteronuclear local field experiment. Chem. Phys. Lett 1997a;280:95–103.

Costa PR, Kocisko DA, Sun BQ, Lansbury PT, Griffin RG. Determination of peptide amide configuration in a model amyloid fibril by solid state NMR. J. Am. Chem. Soc 1997b;119:10487–10493.

Dabbagh G, Weliky DP, Tycko R. Determination of monomer conformations in noncrystalline solid polymers by two-dimensional NMR exchange spectroscopy. Macromolecules 1994;27:6183–6191.

Der-Sarkissian A, Jao CC, Chen J, Langen R. Structural organization of β-synuclein fibrils studied by site-directed spin labeling. J. Biol. Chem 2003;278:37530–37535. [PubMed: 12815044]

Feng X, Eden M, Brinkmann A, Luthman H, Eriksson L, Graslund A, Antzutkin ON, Levitt MH. Direct determination of a peptide torsional angle psi by double-quantum solid state NMR. J. Am. Chem. Soc 1997;119:12006–12007.

Feng X, Lee YK, Sandstrom D, Eden M, Maisel H, Sebald A, Levitt MH. Direct determination of a molecular torsional angle by solid state NMR. Chem. Phys. Lett 1996;257:314–320.

George AR, Howlett DR. Computationally derived structural models of the β-amyloid found in Alzheimer's disease plaques and the interaction with possible aggregation inhibitors. Biopolymers 1999;50:733–741. [PubMed: 10547528]

Goldsbury CS, Wirtz S, Muller SA, Sunderji S, Wicki P, Aebi U, Frey P. Studies on the *in vitro* assembly of $A\beta_{1-40}$: Implications for the search for Aβ fibril formation inhibitors. J. Struct. Biol 2000;130:217–231. [PubMed: 10940227]

Gordon DJ, Balbach JJ, Tycko R, Meredith SC. Increasing the amphiphilicity of an amyloidogenic peptide changes the β-sheet structure in the fibrils from antiparallel to parallel. Biophys. J 2004;86:428–434. [PubMed: 14695285]

Gregory DM, Benzinger TLS, Burkoth TS, Miller-Auer H, Lynn DG, Meredith SC, Botto RE. Dipolar recoupling NMR of biomolecular self-assemblies: Determining inter- and intrastrand distances in fibrillized Alzheimer's β-amyloid peptide. Solid State Nucl. Magn. Reson 1998;13:149–166. [PubMed: 10023844]

Gullion T, Schaefer J. Rotational-echo double-resonance NMR. J. Magn. Reson 1989;81:196–200.

Gullion T, Vega S. A simple magic angle spinning NMR experiment for the dephasing of rotational echoes of dipolar coupled homonuclear spin pairs. Chem. Phys. Lett 1992;194:423–428.

Guo JT, Wetzel R, Ying X. Molecular modeling of the core of Aβ amyloid fibrils. Proteins 2004;57:357–364. [PubMed: 15340923]

Havlin RH, Tycko R. Probing site-specific conformational distributions in protein folding with solid state NMR. Proc. Natl. Acad. Sci. U. S. A 2005;102:3284–3289. [PubMed: 15718283]

Heller J, Kolbert AC, Larsen R, Ernst M, Bekker T, Baldwin M, Prusiner SB, Pines A, Wemmer DE. Solid-state NMR studies of the prion protein H1 fragment. Protein Sci 1996;5:1655–1661. [PubMed: 8844854]

Hing AW, Vega S, Schaefer J. Transferred-echo double-resonance NMR. J. Magn. Reson 1992;96:205–209.

Hohwy M, Jakobsen HJ, Eden M, Levitt MH, Nielsen NC. Broadband dipolar recoupling in the nuclear magnetic resonance of rotating solids: A compensated C7 pulse sequence. J. Chem. Phys 1998;108:2686–2694.

Ishii Y. ^{13}C-^{13}C dipolar recoupling under very fast magic angle spinning in solid state nuclear magnetic resonance: Applications to distance measurements, spectral assignments, and high-throughput secondary-structure determination. J. Chem. Phys 2001;114:8473–8483.

Ishii Y, Balbach JJ, Tycko R. Measurement of dipole-coupled lineshapes in a many-spin system by constant-time two-dimensional solid state NMR with high-speed magic-angle spinning. Chem. Phys 2001;266:231–236.

Ishii Y, Terao T, Kainosho M. Relayed anisotropy correlation NMR: Determination of dihedral angles in solids. Chem. Phys. Lett 1996;256:133–140.

Jaroniec CP, Filip C, Griffin RG. 3D TEDOR NMR experiments for the simultaneous measurement of multiple carbon-nitrogen distances in uniformly ^{13}C, ^{15}N-labeled solids. J. Am. Chem. Soc 2002a; 124:10728–10742. [PubMed: 12207528]

Jaroniec CP, MacPhee CE, Astrof NS, Dobson CM, Griffin RG. Molecular conformation of a peptide fragment of transthyretin in an amyloid fibril. Proc. Natl. Acad. Sci. U. S. A 2002b;99:16748–16753. [PubMed: 12481032]

Jaroniec CP, MacPhee CE, Bajaj VS, McMahon MT, Dobson CM, Griffin RG. High-resolution molecular structure of a peptide in an amyloid fibril determined by magic angle spinning NMR spectroscopy. Proc. Natl. Acad. Sci. U. S. A 2004;101:711–716. [PubMed: 14715898]

Jayasinghe SA, Langen R. Identifying structural features of fibrillar islet amyloid polypeptide using site-directed spin labeling. J. Biol. Chem 2004;279:48420–48425. [PubMed: 15358791]

Jimenez JL, Nettleton EJ, Bouchard M, Robinson CV, Dobson CM, Saibil HR. The protofilament structure of insulin amyloid fibrils. Proc. Natl. Acad. Sci. U. S. A 2002;99:9196–9201. [PubMed: 12093917]

Kammerer RA, Kostrewa D, Zurdo J, Detken A, Garcia-Echeverria C, Green JD, Muller SA, Meier BH, Winkler FK, Dobson CM, Steinmetz MO. Exploring amyloid formation by a *de novo* design. Proc. Natl. Acad. Sci. U. S. A 2004;101:4435–4440. [PubMed: 15070736]

Lange A, Becker S, Seidel K, Giller K, Pongs O, Baldus M. A concept for rapid protein-structure determination by solid state NMR spectroscopy. Angew. Chem.-Int. Edit 2005;44:2089–2092.

Lansbury PT, Costa PR, Griffiths JM, Simon EJ, Auger M, Halverson KJ, Kocisko DA, Hendsch ZS, Ashburn TT, Spencer RGS, Tidor B, Griffin RG. Structural model for the β-amyloid fibril based on interstrand alignment of an antiparallel-sheet comprising a C-terminal peptide. Nat. Struct. Biol 1995;2:990–998. [PubMed: 7583673]

Laws DD, Bitter HML, Liu K, Ball HL, Kaneko K, Wille H, Cohen FE, Prusiner SB, Pines A, Wemmer DE. Solid state NMR studies of the secondary structure of a mutant prion protein fragment of 55 residues that induces neurodegeneration. Proc. Natl. Acad. Sci. U. S. A 2001;98:11686–11690. [PubMed: 11562491]

Lazo ND, Downing DT. Amyloid fibrils may be assembled from β-helical protofibrils. Biochemistry 1998;37:1731–1735. [PubMed: 9492738]

Li LP, Darden TA, Bartolotti L, Kominos D, Pedersen LG. An atomic model for the pleated β-sheet structure of Aβ amyloid protofilaments. Biophys. J 1999;76:2871–2878. [PubMed: 10354415]

Long HW, Tycko R. Biopolymer conformational distributions from solid state NMR: β-helix and 3_{10}-helix contents of a helical peptide. J. Am. Chem. Soc 1998;120:7039–7048.

McDermott AE, Creuzet F, Gebhard R, Vanderhoef K, Levitt MH, Herzfeld J, Lugtenburg J, Griffin RG. Determination of internuclear distances and the orientation of functional-groups by solid state NMR: Rotational resonance study of the conformation of retinal in bacteriorhodopsin. Biochemistry 1994;33:6129–6136. [PubMed: 8193126]

Mehta MA, Gregory DM, Kiihne S, Mitchell DJ, Hatcher ME, Shiels JC, Drobny GP. Distance measurements in nucleic acids using windowless dipolar recoupling solid state NMR. Solid State Nucl. Magn. Reson 1996;7:211–228. [PubMed: 9050159]

Meier BH, Earl WL. Excitation of multiple quantum transitions under magic angle spinning conditions: Adamantane. J. Chem. Phys 1986;85:4905–4911.

Michal CA, Jelinski LW. REDOR 3D: Heteronuclear distance measurements in uniformly labeled and natural abundance solids. J. Am. Chem. Soc 1997;119:9059–9060.

Naito A, Kamihira M, Inoue R, Saito H. Structural diversity of amyloid fibril formed in human calcitonin as revealed by site-directed ^{13}C solid state NMR spectroscopy. Magn. Reson. Chem 2004;42:247–257. [PubMed: 14745805]

Oyler NA, Tycko R. Absolute structural constraints on amyloid fibrils from solid state NMR spectroscopy of partially oriented samples. J. Am. Chem. Soc 2004;126:4478–4479. [PubMed: 15070340]

Perutz MF, Johnson T, Suzuki M, Finch JT. Glutamine repeats as polar zippers: Their possible role in inherited neurodegenerative diseases. Proc. Natl. Acad. Sci. U. S. A 1994;91:5355–5358. [PubMed: 8202492]

Petkova AT, Buntkowsky G, Dyda F, Leapman RD, Yau WM, Tycko R. Solid state NMR reveals a pH-dependent antiparallel β-sheet registry in fibrils formed by a β-amyloid peptide. J. Mol. Biol 2004;335:247–260. [PubMed: 14659754]

Petkova AT, Ishii Y, Balbach JJ, Antzutkin ON, Leapman RD, Delaglio F, Tycko R. A structural model for Alzheimer's β-amyloid fibrils based on experimental constraints from solid state NMR. Proc. Natl. Acad. Sci. U. S. A 2002;99:16742–16747. [PubMed: 12481027]

Petkova AT, Leapman RD, Guo ZH, Yau WM, Mattson MP, Tycko R. Self-propagating, molecular-level polymorphism in Alzheimer's β-amyloid fibrils. Science 2005;307:262–265. [PubMed: 15653506]

Reif B, Hohwy M, Jaroniec CP, Rienstra CM, Griffin RG. NH-NH vector correlation in peptides by solid state NMR. J. Magn. Reson 2000;145:132–141. [PubMed: 10873504]

Saito H. Conformation-dependent ^{13}C chemical-shifts: A new means of conformational characterization as obtained by high-resolution solid state ^{13}C NMR. Magn. Reson. Chem 1986;24:835–852.

Schmidt-Rohr K. A double-quantum solid state NMR technique for determining torsion angles in polymers. Macromolecules 1996a;29:3975–3981.

Schmidt-Rohr K. Torsion angle determination in solid ^{13}C-labeled amino acids and peptides by separated-local-field double-quantum NMR. J. Am. Chem. Soc 1996b;118:7601–7603.

Serpell LC, Smith JM. Direct visualisation of the β-sheet structure of synthetic Alzheimer's amyloid. J. Mol. Biol 2000;299:225–231. [PubMed: 10860734]

Sharpe S, Kessler N, Anglister JA, Yau WM, Tycko R. Solid state NMR yields structural constraints on the V3 loop from HIV-1 gp120 bound to the 447-52d antibody Fv fragment. J. Am. Chem. Soc 2004;126:4979–4990. [PubMed: 15080704]

Siemer AB, Ritter C, Ernst M, Riek R, Meier BH. High-resolution solid state NMR spectroscopy of the prion protein Het-s in its amyloid conformation. Angew. Chem. Int. Ed 2005;44:2441–2444.

Spera S, Bax A. Empirical correlation between protein backbone conformation and Cα and Cβ ^{13}C nuclear magnetic resonance chemical shifts. J. Am. Chem. Soc 1991;113:5490–5492.

Sunde M, Blake CCF. From the globular to the fibrous state: Protein structure and structural conversion in amyloid formation. Q. Rev. Biophys 1998;31:1–39. [PubMed: 9717197]

Takegoshi K, Imaizumi T, Terao T. One- and two-dimensional ^{13}C-^{1}H/^{15}N-^{1}H dipolar correlation experiments under fast magic-angle spinning for determining the peptide dihedral angle phi. Solid State Nucl. Magn. Reson 2000;16:271–278. [PubMed: 10928631]

Torok M, Milton S, Kayed R, Wu P, McIntire T, Glabe CG, Langen R. Structural and dynamic features of Alzheimer's Aβ peptide in amyloid fibrils studied by site-directed spin labeling. J. Biol. Chem 2002;277:40810–40815. [PubMed: 12181315]

Tycko R. Progress towards a molecular-level structural understanding of amyloid fibrils. Curr. Opin. Struct. Biol 2004;14:96–103. [PubMed: 15102455]

Tycko R, Dabbagh G. Measurement of nuclear magnetic dipole-dipole couplings in magic angle spinning NMR. Chem. Phys. Lett 1990;173:461–465.

Tycko R, Dabbagh G. Nuclear magnetic resonance crystallography: Molecular orientational ordering in three forms of solid methanol. J. Am. Chem. Soc 1991;113:3592–3593.

Tycko R, Dabbagh G. A simple theory of ^{13}C nuclear spin diffusion in organic solids. Isr. J. Chem 1992;32:179–184.

Tycko R, Dabbagh G, Mirau PA. Determination of chemical shift anisotropy lineshapes in a two-dimensional magic-angle-spinning NMR experiment. J. Magn. Reson 1989;85:265–274.

Tycko R, Ishii Y. Constraints on supramolecular structure in amyloid fibrils from two-dimensional solid state NMR spectroscopy with uniform isotopic labeling. J. Am. Chem. Soc 2003;125:6606–6607. [PubMed: 12769550]

Weliky DP, Bennett AE, Zvi A, Anglister J, Steinbach PJ, Tycko R. Solid state NMR evidence for an antibody-dependent conformation of the V3 loop of HIV-1 gp120. Nat. Struct. Biol 1999;6:141–145. [PubMed: 10048925]

Weliky DP, Dabbagh G, Tycko R. Correlation of chemical bond directions and functional group orientations in solids by two-dimensional NMR. J. Magn. Reson. Ser. A 1993;104:10–16.

Weliky DP, Tycko R. Determination of peptide conformations by twodimensional magic angle spinning NMR exchange spectroscopy with rotor synchronization. J. Am. Chem. Soc 1996;118:8487–8488.

Williams AD, Portelius E, Kheterpal I, Guo JT, Cook KD, Xu Y, Wetzel R. Mapping Aβ amyloid fibril secondary structure using scanning proline mutagenesis. J. Mol. Biol 2004;335:833–842. [PubMed: 14687578]

Wishart DS, Sykes BD, Richards FM. Relationship between nuclear magnetic resonance chemical shift and protein secondary structure. J. Mol. Biol 1991;222:311–333. [PubMed: 1960729]

Yao XL, Hong M. Structure distribution in an elastin-mimetic peptide $(VPGVG)_3$ investigated by solid state NMR. J. Am. Chem. Soc 2004;126:4199–4210. [PubMed: 15053609]

Figure 1:
^{13}C NMR secondary shifts (*i.e.*, differences between observed chemical shifts and random coil shifts) for amyloid fibrils formed by $A\beta_{16\text{-}22}$ (N-acetyl-KLVFFAE-amide). Negative secondary shifts for β-carbons and carbonyl carbons and positive secondary shifts for β-carbons indicate a β-strand containing residues 17-21 (Balbach *et al*., 2000).

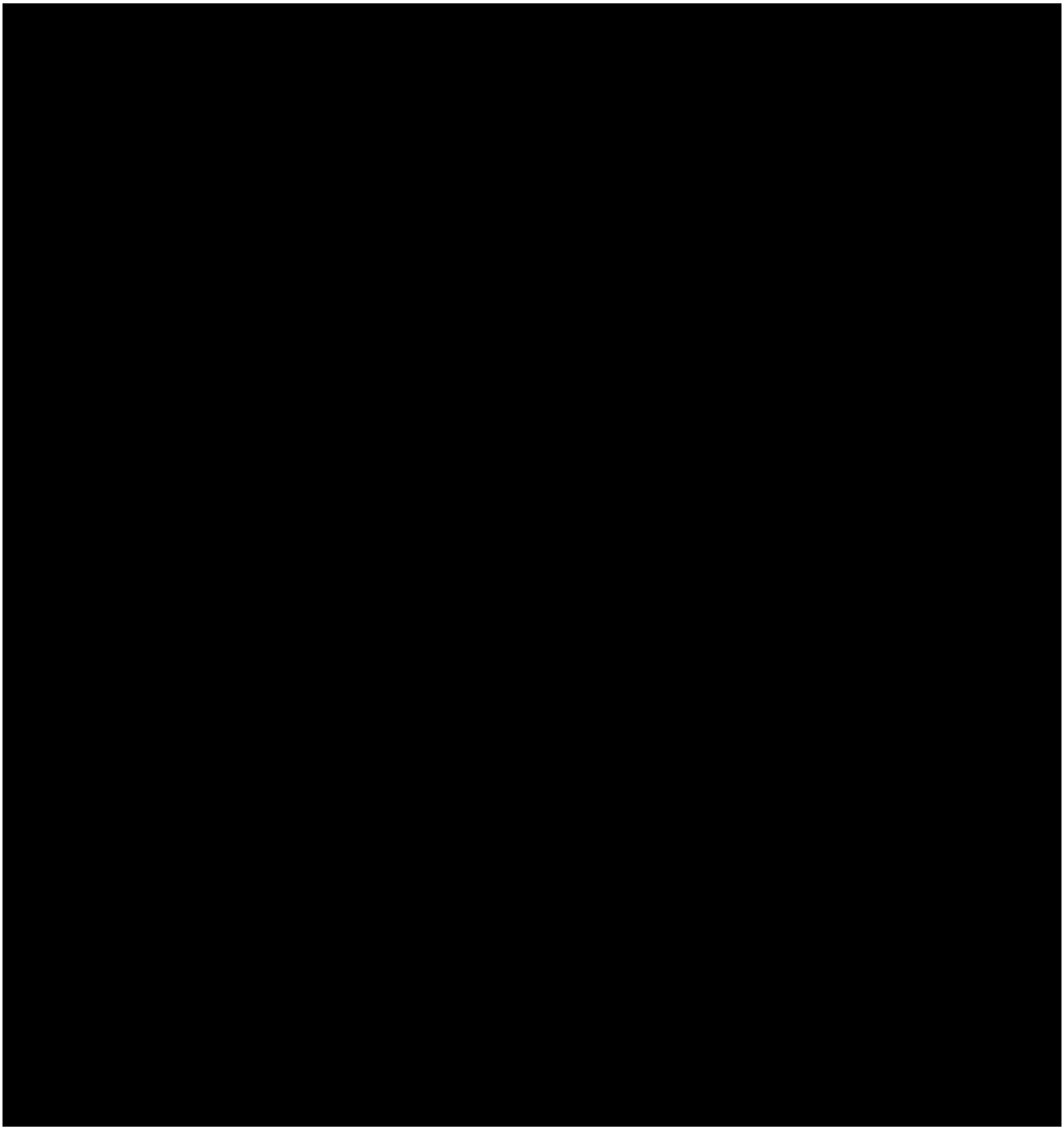

Figure 2:
Two-dimensional ^{13}C NMR spectra of $A\beta_{1-40}$ fibrils in lyophilized form, obtained with magic-angle spinning under conditions that produce strong crosspeaks for directly bonded ^{13}C pairs (Ishii, 2001; Petkova *et al*., 2002). Full spectra (a,c) and expansions of the aliphatic regions (b,d) are shown for fibrils that are uniformly ^{15}N,^{13}C-labeled at A2, D7, G9, Y10, V12, and M35 (a,b) or F10, D23, V24, K28, G29, A30, and I31 (c,d). Solid and dashed lines indicate crosspeak connectivities used for resonance assignment. Note the broad crosspeaks for A2 and D7, which support the existence of a disordered N-terminal segment in $A\beta_{1-40}$ fibrils. Spectra were recorded in a 9.4 T field, with magic-angle spinning at approximately 23 kHz.

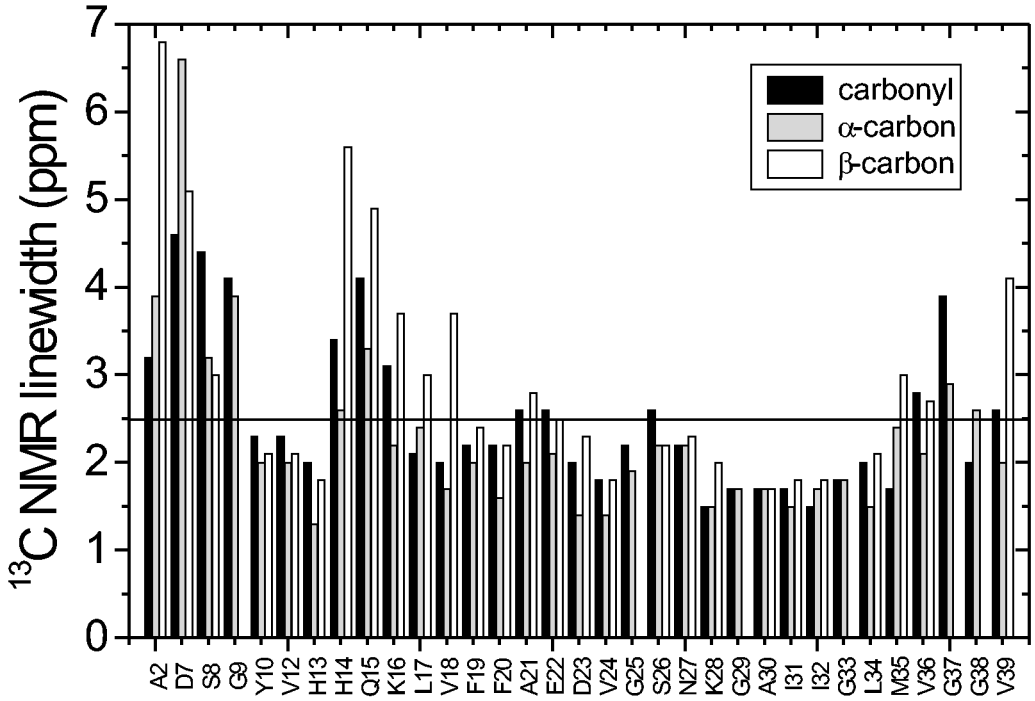

Figure 3:
^{13}C NMR linewidths (full width at half maximum) extracted from two-dimensional spectra as in Fig. 2. These data indicate conformational disorder in the N-terminal segment, in the vicinity of Q15, and (to a lesser extent) in residues 35-39. Other residues are well ordered.

Figure 4:
Experimental constraints on intermolecular distances in $A\beta_{1\text{-}40}$ fibrils, using the fpRFDR-CT technique (Balbach *et al*., 2002; Ishii *et al*., 2001) to measure ^{13}C-^{13}C nuclear magnetic dipole-dipole couplings in samples that are ^{13}C labeled at single sites in V12, A30, or V39. Simulations for linear chains of ^{13}C nuclei with nearest-neighbor spacings from 4.0 Å to 7.0 Å are shown. These data indicate that the labeled residues participate in in-register parallel β-sheets. Data were obtained in 9.4 T field, with magic-angle spinning at 20.0 kHz.

Figure 5:
Measurements of intermolecular dipole-dipole couplings between ^{15}N labels at backbone amide sites and ^{13}C labels at backbone carbonyl sites in amyloid fibrils formed by $A\beta_{16-22}$ with either acetyl (circles, downward triangles) or octanoyl (upward triangles, squares) groups at the N-terminus. These measurements use the REDOR solid state NMR technique (Anderson *et al*., 1995; Gullion and Schaefer, 1989). Fibrils are formed from mixtures of molecules that are ^{15}N-labeled at A21 and molecules that are ^{13}C-labeled at L17 (circles, squares) or F20 (triangles), with an approximate 1.6:1.0 ratio of ^{15}N-labeled to ^{13}C-labeled molecules. Curves are simulations in which the labeled residues are hydrogen bonded in parallel (solid line) or antiparallel (dashed line) β-sheets, or shifted from hydrogen bonded positions by one residue in parallel (dash-dotted line) or antiparallel (dotted line) β-sheets. These data indicate an antiparallel β-sheet structure with hydrogen bonds between residues 17+k and 21-k (k = 0, 1, 2, 3) for the acetyl peptide, and an in-register parallel β-sheet structure for the octanoyl peptide (Gordon *et al*., 2004). Data were obtained in a 9.4 T field, with magic-angle spinning at 5.00 kHz.

Figure 6:
Proton-mediated two-dimensional ^{13}C-^{13}C exchange spectra of $A\beta_{11-25}$ fibrils grown at pH 7.4 (a) or pH 2.4 (b), with uniform ^{15}N and ^{13}C labeling of V18, F19, F20, and A21. Strong crosspeaks between α-carbon chemical shifts of V18 and α-carbon chemical shifts of either F19 (a) or A21 (b) indicate the hydrogen bond registry in antiparallel β-sheets (Petkova *et al*., 2004; Tycko and Ishii, 2003). At pH 7.4, residue 17+k is hydrogen bonded to residue 20-k. At pH 2.4, residue 17+k is hydrogen bonded to residue 22-k. Spectra were recorded in a 14.1 T field, with magic-angle spinning at 21.40 kHz.

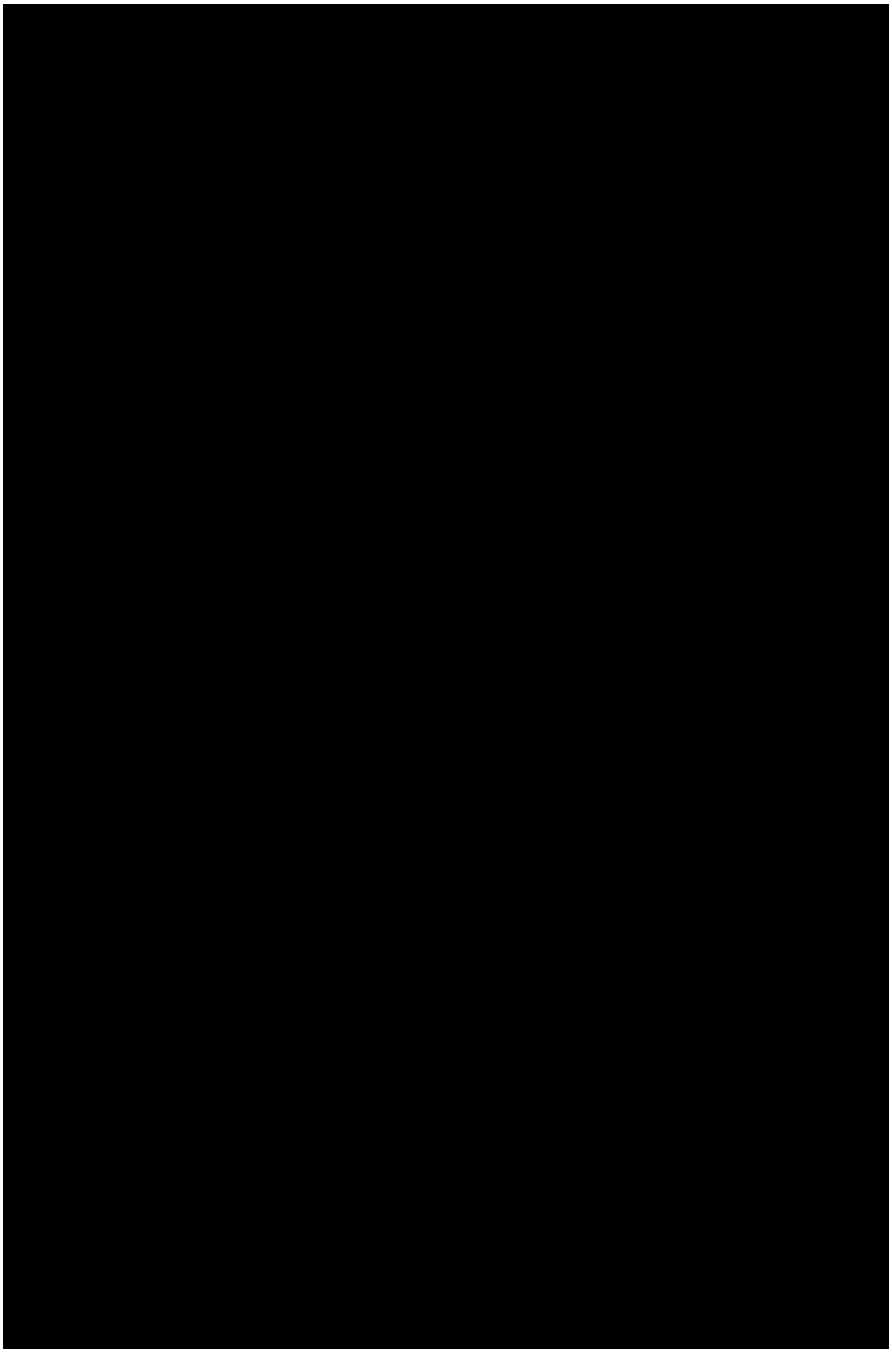

Figure 7:
(a) Two-dimensional ^{13}C-^{13}C exchange spectra of $A\beta_{1\text{-}40}$ fibrils, prepared with uniform ^{15}N and ^{13}C labeling of K16, F19, A21, E22, I32, and V36, obtained with a 500 ms exchange period. (b) One-dimensional slices taken at positions indicated by the dashed lines in the two-dimensional spectrum. The slice at the chemical shift of F19 aromatic carbons shows crosspeaks at the chemical shifts of V36 aliphatic carbons (dotted lines) and I32 aliphatic carbons (dotdashed lines). These crosspeaks indicate contacts between aromatic and aliphatic sidechains, placing constraints on quaternary structure. The spectrum was recorded in a 14.1 T field, with magic-angle spinning at 18.00 kHz.

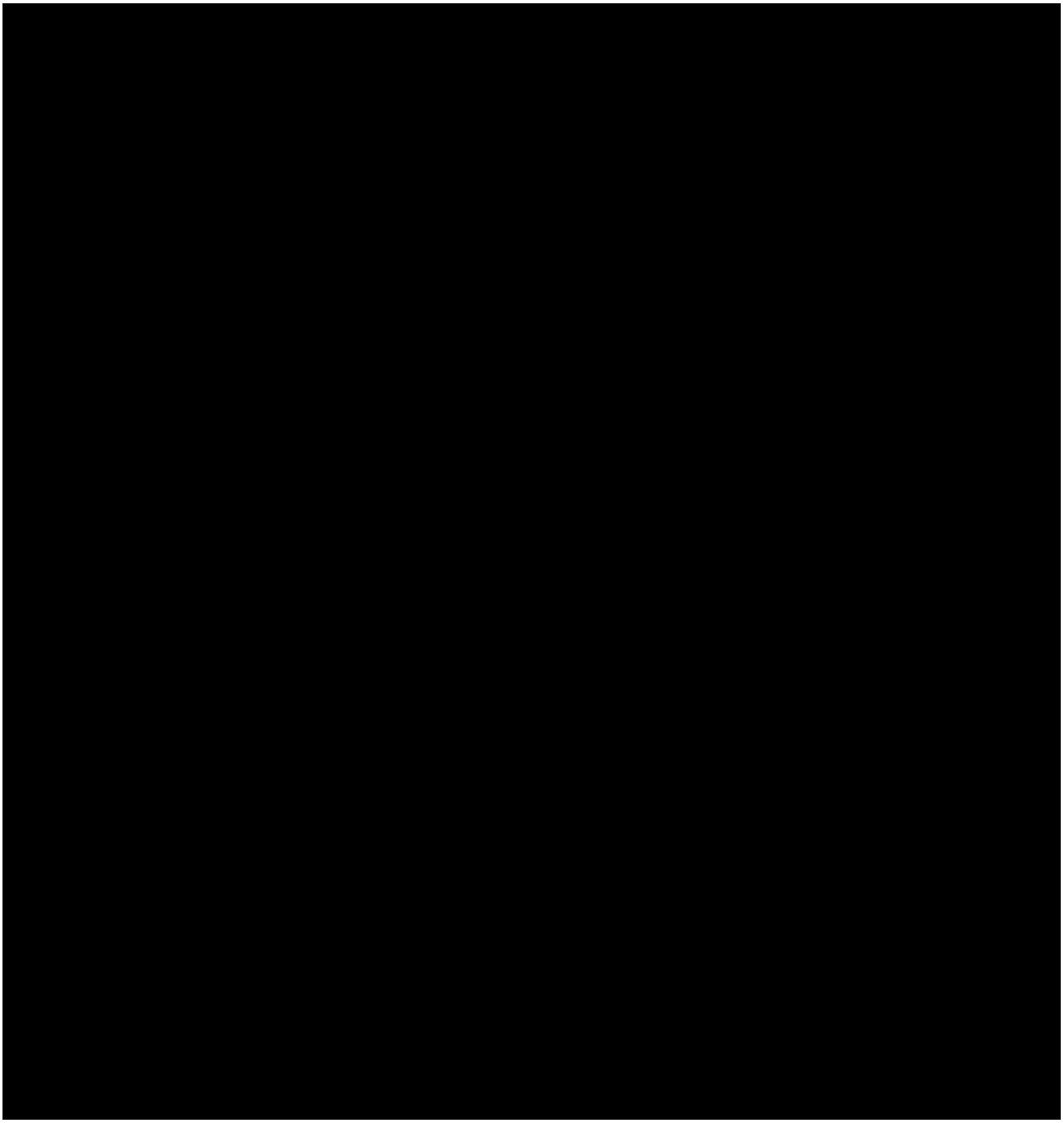

Figure 8:
(a) Two-dimensional ^{15}N-^{13}C TEDOR spectrum of $A\beta_{1-40}$ fibrils, prepared with uniform ^{15}N and ^{13}C labeling of I31, G33, M35, G37, and V39, obtained with 5.745 ms ^{15}N-^{13}C recoupling periods (Jaroniec *et al*., 2002a). Crosspeaks indicate the proximity of particular ^{13}C-labeled backbone and sidechain sites to ^{15}N-labeled backbone amide sites. (b) One-dimensional slices taken at the ^{15}N chemical shift of G33, indicated by the dashed line in the two-dimensional spectrum, for samples grown from labeled $A\beta_{1-40}$ (top) and from a 2:1 mixture of unlabeled and labeled $A\beta_{1-40}$. The reduced amplitude of the M35 methyl crosspeak relative to the G33 carbonyl crosspeak in the isotopically diluted sample indicates that the M35 methyl/G33 amide

contact is primarily intermolecular and therefore represents a quaternary constraint. Spectra were recorded in a 14.1 T field, with magic-angle spinning at 11.140 kHz.